Chapter 1

Introduction and literature review

Nature has always been an invaluable source of inspiration for technological progress. Great scientific revolutions were started by the work of men such as Leonardo da Vinci and Galileo Galilei, who were able to learn from nature and apply their knowledge most effectively. The process of transferring the ingenious solutions evolved by some species into engineered devices is now an established and autonomous discipline known as *biomimetics*.

Due to advances in the fabrication technologies of nanometer-scale optical devices, biomimetics has expanded into the field of non-classical optics. This gives an opportunity for engineers and zoologists to learn from nature in a mutually beneficial partnership. Engineers can draw inspiration from the ways in which Nature produces fascinating optical effects and zoologists can apply the quantitative theoretical methods developed in optical engineering to understand the phenomenology of their specimens. The development of expertise brought about by this interaction has already resulted in commercially available products. The surface of some optical discs for data storage and certain surface-relief volume phase holograms share the designs and functionality of the microstructures found in the eye of moths and on the wings of butterflies.

Visual appearance is one of the areas in which nature has evolved smart optical solutions. Through interference of light reflected or diffracted by minute features, many organisms are able to generate structural colour. Different optical effects are generated by arrangements of biomaterial on the surface of various organisms. Amongst the many examples of structural colour found in nature, the beauty of the intense chromatic display of butterflies has strongly captured the interest of researchers. The history of the investigations carried out on one species of tropical butterfly, *Morpho rhetenor*, has been particularly long, no doubt because of the striking brilliance of the blue color shining from its wings. The intricate microstructure that covers the wings of this butterfly achieves, in the short wavelength regime of the visible spectrum, an extremely high reflection with a very large angular spread of the back-scattered light using a low index of refraction.

This chapter presents an introduction to the work reported in later chapters of this thesis. The motivation for this study and a review of the material published by other scientists on subjects inherent to the development of the thesis are therein discussed. This literature review will have the following structure: first structural colour is briefly introduced with a section specific to butterflies; published models of the optical properties of the wings of butterflies are reviewed and their agreement with experimental data is discussed; successively, the modelling of multilayers and diffractive structures is discussed in order of complexity of the methods; an overview of photonic crystals is then presented and particular attention is devoted in three respective sections to modelling techniques, two-dimensional structures fabricated by layering of materials, and three-dimensional photonic crystals designed to operate in the visible and near-infrared regimes; finally, recent advances in spectroscopy are discussed.

1.1 Motivation

The intention of this study has been to investigate the microstructure found on the wings of *Morpho rhetenor* with the help of experimental and theoretical methods used at the forefront of research in the field of quantum optics. The morphology of the microstructure and its optical phenomenology suggest that an understanding of the mechanisms involved in the production of the structural colour requires the use of more advanced theoretical models than previously thought.

Over more than a century, several models of the interaction of light with the natural materials that produce structural colour have been proposed. With the need to find more accurate and complete descriptions, their complexity has progressively increased, passing from one-dimensional models which considered the *Morpho* microstructure as a stack of thin-films (multilayers), to the latest multilevel grating model. Advances in optical engineering which are unrelated to biology or zoology, have provided the theoretical means for this evolution. Progress in the development of new computational methods for diffractive optics has been fuelled by successful commercial applications during the last two decades in the fields of diffractive optics and photonics.

A detailed characterization of the scattering of light by the *Morpho* microstructure was necessary to obtain a more complete view of its phenomenology and to assess whether the complex modelling techniques used in diffractive optics are needed to explain all its properties. Technological advances in photonics, namely in the field of optical fibres, have made new sources of coherent, white light available. For this study of the *Morpho* microstructure, these sources were implemented in a novel experimental method for the investigation of the scattering of materials structured on a nanometer-scale via visible to near infrared spectroscopy.

The choice to study *Morpho rhetenor* instead of any other organism exhibiting structural coloration was dictated by the interest provoked by its optical properties in new fields of optical engineering, and also by the avail-

ability of accurate morphological information. The surface covering the wings of the butterfly which is responsible for its structural coloration, is very similar to a new class of optical materials currently being developed, namely the photonic crystals (PCs) or photonic bandgap materials. Understanding the interaction of light with the surface of the butterfly wing could represent a step forward in the design of new PCs.

Progress in microelectronics, optoelectronics and photonics has also supported the development of fabrication technologies capable of structuring dielectric thin-films on a nanometer scale. In the present study novel diffractive structures and PCs have been produced using these state-of-the-art fabrication processes. The design of these structures was inspired by the *Morpho* microstructure. Using low-index materials the fabricated devices yielded high diffraction efficiencies and strong polarisation effects, which cannot be obtained with the traditional designs for dielectric diffractive structures.

1.2 Structural colour

The study of structural colour is old. Observations of optical interference effects have been reported by illustrious scientists, whose ingenuity has laid the foundations of modern science. In a time when the wonders of nanotechnologies were not conceivable, those researchers turned to nature and used their intuition to identify, via their phenomenology, optical microstructures which they could not possibly see. Hooke [1] in 1665 when considering the optical properties of silverfish (*Ctenoplisma* sp.) observed:

> ... the appearance of so many several shells or shields that cover the whole body, every one of these shells are covered or tiled over with a multitude of transparent scales, which, from the multiplicity of their reflecting surfaces, make the whole animal a perfect pearl colour.

Newton dedicated his *Second book of Opticks* [2] to the optics of thin transparent bodies and in one of his propositions he observed:

> [...] The finely colour'd Feathers of some Birds, and particularly those of Peacocks Tails, do, in the very same part of the Feather, appear of several Colours in several Positions of the eye, after the very same manner that thin Plates were found to do [...] and therefore their Colours arise from the thinness of the transparent parts of the Feathers; that is, from the slenderness of the very fine Hairs, or *Capillamenta*, which grow out of the sides of the grosser lateral Branches or Fibres of those Feathers.

Acknowledgment of the intrinsic relation between structural colour and the interaction of light with microscopic objects emerged in those early days, together with the scientists' new found interest in the phenomena of interference, refraction and reflection, and understanding of the nature of light.

1.2.1 General literature

Colour has always been a privileged subject of study for thinkers who devoted themselves to natural sciences; we have already mentioned the famous examples of Hooke and Newton. In recent years though, the study of colour has become a scientific discipline *per se*, intimately related to the fields of Physics, Chemistry, Biology, Materials Science and Engineering. Monographs are now dedicated to this subject, like the book by Tilley [3].

This continued and ever increasing interest, supported by the introduction of new investigation techniques, such as electron microscopy, has made it possible to discover countless examples of structural colour in Nature. Feathers of many birds, like parrots and peacocks, scales of fishes, hair of sea mice, retinal tissue of cats, and wings of butterflies are all examples of a phenomenon occurring across the animal kingdom. The mechanisms for the production of colour are varied [4] and sometimes mixed [4, 5]. The shapes in which dielectrics are structured in animals are diverse and the history of their evolution very long, since structures capable of reflecting vivid, iridescent colours have been found in fossils up to 515 million years old [6].

The perception of colour is a complex matter involving generation of a physiological *stimulus* by means of light of a certain spectral content and intensity [3, 7]. The subjectivity of this process equally affects the study of structural colour. Several natural devices capable of creating similar stimuli were found.

Structural colours are sometimes called *metallic* or *iridescent* colours, these names suggested by the very high intensity and broad bandwidth of light in one case, and by the change in spectral content with changing angle (iridescence) in the other. A well established definition for any of these terms does not exist. It is safe to say the phenomena addressed with these names all rely on the presence of a distribution of indexes of refraction in the investigated object.

Classification of the occurring structures might be an important issue for zoologists because it can help them establish phylogenies and interspecific relations, such as convergence and divergence, by looking at functional and structural homologues. Attempts have been made at classifying them by chromatic appearance, function, building substances, or physical mechanisms involved. A vast and very popular work by Fox [4] reviews the occurrence of colour in many species and makes a distinction between whites, *Tyndall* blues and iridescent colours. Fox proposes that these are due, respectively, to dense, inhomogeneous colloidal systems, randomly ordered scatterers (*Tyndall* scattering), and multilayer systems. Fox also considers diffraction as a possible mechanism for the generation of colour. Land [8], who limited his study to multilayer structures in animals, classifies the systems with respect to the materials and relative indexes of refraction involved. Parker [6] classifies the structures found in invertebrates by the mechanism behind the generation of the structural colour, thus naming three classes: *thin-film reflectors*, *diffraction gratings* and scattering structures. Parker also adds though, that often all of these mechanisms apply to one sample and classification becomes a rather academic exercise.

A wide variety of diffractive structures is found in Nature. These are specialized devices functioning as reflectors in most cases, but also as transmitters. Depending on their function, they may have different periods, some of sizes smaller than the wavelength of the relevant radiation (zero-order structures [9]), or be periodic along two directions on the corrugated surface [10]. Colour can also be generated by a three-dimensional distribution of dielectric material such as is found in crystal lattices. Extremely regular lattices, in fact face-centered cubic crystals of inverted spheres, occur in iridescent butterflies [11, 12]. Similarly, structural colour is produced by opals [13], iridescent stones made of ordered grains of amorphous silica, which have an internal structure periodic in three dimensions. Often the term *opalescence* is used in this case instead of iridescence. Naturally, we expect the relevant interaction between light and three-dimensional structures to take place in the inside of the samples, but it must be emphasized that this also applies to surface diffractive structures. Even in specimens which we regard as surface, one- or two-dimensional structures, the electromagnetic field often penetrates deeply inside the periodic arrangement of dielectric material and the chromatic effect results from the extension of the waves deep within the structure. For this reason, they must be regarded as volume diffractive structures rather than surface ones. The cat tapetum [8] or the hair of the sea mouse [14] are examples of systems in which the iridescence is the result of interdependent diffraction and interference processes.

The striking intensity and amazing effects of structural colour in Nature are achieved with materials, and control over the geometries, that by some human standards would be regarded as rather limited. It is interesting to consider which indexes of refraction are available to animals to produce their striking displays. Land [8] has named those listed in table 1.1 as the most commonly occurring. The occurring contrasts in index of refraction are less than 1.83 and therefore only a small reflection can take place at individual boundaries between two materials for small angles of incidence.

Table 1.1: Materials composing most animal microstructures [8].

Index of refraction	Substance
1	air
1.33	water, cytoplasm
1.56	dried protein (*e.g.* keratin) or chitin
1.83	guanine

1.2.2 Butterflies

Many tropical butterflies display magnificent colours which are results of an interaction of light with the complex microstructure of the cuticle which covers their wings. Structural colour is not limited to tropical specimens and is also found in lepidopterans from temperate climatic regions.

The wings of lepidopterans are covered with a layer of *ground scales* in a fashion comparable to the tiling of roofs. A second layer of scales, called *cover scales*, can overlay the first one. The cover scales are mainly responsible for the structural colour and different species have different areas of coverage with iridescent scales. All butterfly and moth scales share the same basic architecture. A scale is essentially a flattened sac with a stalk that fits into a socket in the wing. The bottom layer of this sac is mostly featureless, while the top is ridged as a diffraction grating (see figure 1.1). The overall shape is elongated and the structure appears as if it had been extruded from the cell in the stem. The ridges are kept at a constant distance from each other by a regular series of cross-ribs and are supported from the bottom via pillars or trabeculae. The space between top and bottom layer can be empty, filled with amorphously distributed material, or alternating layers of cuticle and air, or a close-packed hexagonal structure. The ridges are usually finished with a series of longitudinally overlapping, slanted lamellae, which angle down either side of the ridge. At the bottom of the ridge the lamellae are replaced by a series of very fine vertical folds: the microribs. A cross-section perpendicular to the ridges often reveals a pine-tree shape, with alternating layers of cuticle and interstitial space. The lower parts of the scale usually contain pigment

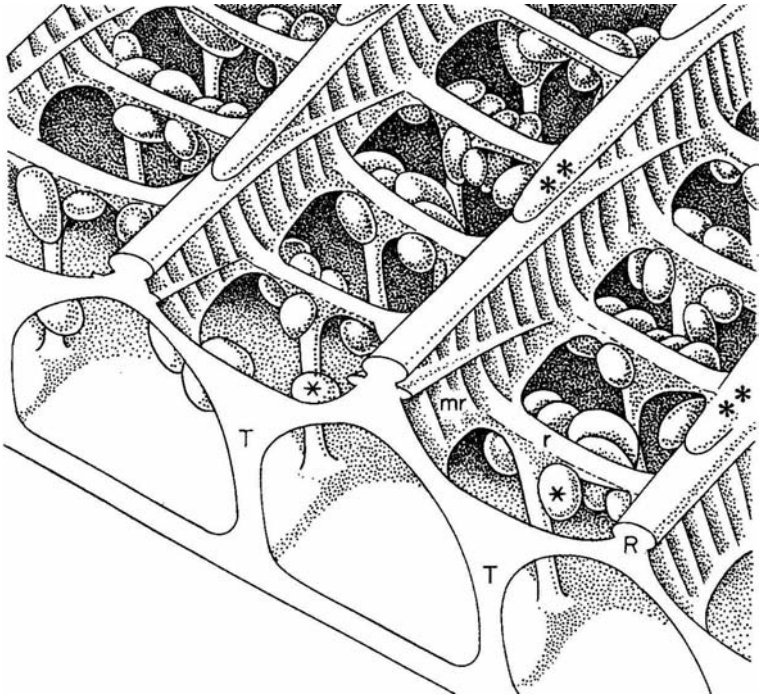

Figure 1.1: Schematic of typical butterfly scale [12]. Note marked fundamental components: trabeculae (T), ridges (R), lamellae (∗∗), ribs (r), and microribs (mr). Pigment granules (∗) are also represented, although they do not occur in all species.

either isolated in granules or diffused throughout. This is the general pattern for iridescent scales, which is then individually differentiated in size or grade of development of the various parts. Ghirardella [11, 12, 15] has extensively studied this subject for many years with a biologist's eye.

Early researchers introduced a distinction amongst iridescent butterflies and named two types [4, 15, 16]: *Morpho* type or class I and *Urania* type or class II. The structures included in the first class are characterised by a significant size of the pine-tree shape of the ridges with respect to their periodicity in the plane of the scale, the latter typically shorter than $1\mu m$. In the structures of the second class the lamellae are not very large, the horizontal periodicity is several microns, and the most important feature of the scale is a more or less corrugated multilayer substrate. Although these classes encompass only some of the iridescent scales of lepidopterans

they have polarised the interest of the scientific community and have become preferred subjects of investigation. Some of the class I butterflies which have been studied are: *Morpho amathonte* [15], *M. didius* [17], *M. menelaus* [15, 18], *M. rhetenor* [17], *Eurema lisa* [19], *Colias euritheme* [12], and *Caligo uranus* [15]. Class II instead comprises *Papilio blumei* [20], *P. karna* [21], *P. palinurus* [5, 11, 16, 21], *P. ulysses* [17], and *Urania ripheus* [4]. Figures 1.2 and 1.3 show transmission electron microscope (TEM) views of the cross-section of scales for class I and II, respectively.

A third class had been added recently to include specimens in which an ordered three-dimensional lattice of cuticle occurs [22].

Despite the large number of studies on the subject of structural colour amongst butterflies, only a few scientists have reported quantitative characterisations of the optical properties of the scales. Huxley [21] reported measurements of the specular reflectance of the wing in two species of butterflies of the second class for unpolarised light at wavelengths between 390 and 700nm and incident at several angles. For the same samples, spectra of the total back-scattered light at normal incidence were also measured and

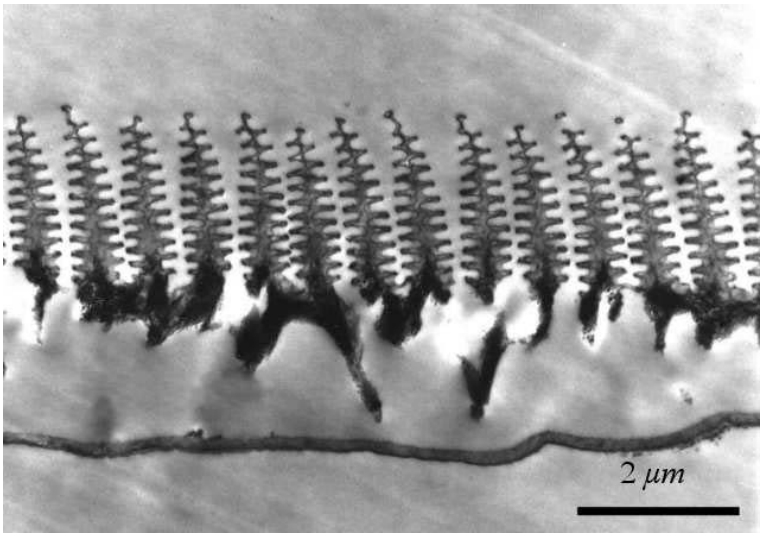

Figure 1.2: Scale of *Morpho rhetenor* butterfly: TEM micrograph of a cross-section [17].

the variation of the wavelength of the reflectance peak with changing angle of incidence was analysed. Ghirardella *et al.* [19] studied the variation of the reflectance peak with changing angle of incidence, but for *Eurema lisa*, a species of the first class. A calibrated measurement of the reflectance of *Papilio blumei*, a class II butterfly, for normally incident light at wavelengths over the $500 - 1450nm$ range, was reported by Tada *et al.* [20]. Vukusic *et al.* [17] published the most complete set of optical measurements on the wings of butterflies to date. For two class I specimens (*Morpho rhetenor* and *Morpho didius*), Vukusic *et al.* measured the scattering in every direction in the plane of incidence (*i.e.* forward and backward scattering) by a single scale for normally incident light of $488nm$ wavelength and both polarisations. Vukusic *et al.* also reported on the reflection from single scales at specific wavelengths throughout the visible spectrum for normally incident light and both polarisations. Their work included investigations into the reflection and transmission from wing areas which included several scales for the whole 200–$700nm$ spectrum, for normal incidence and TM polarisation.

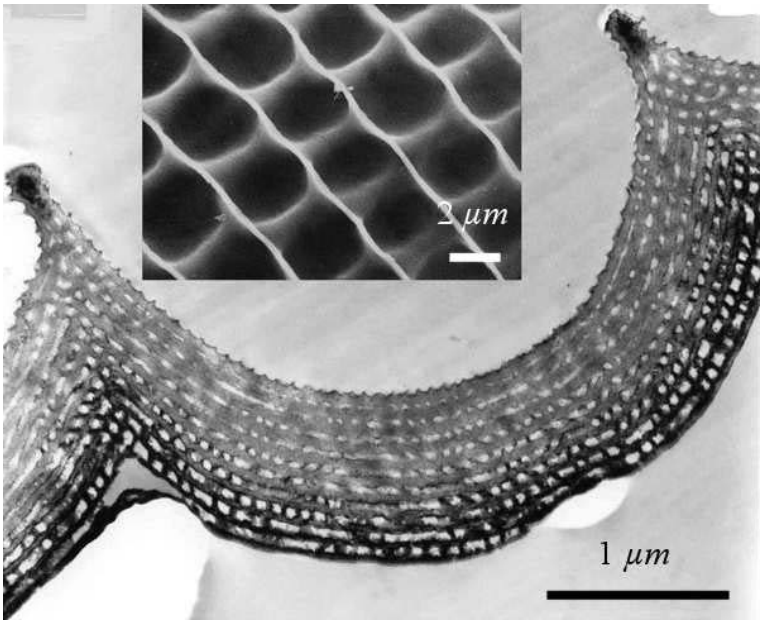

Figure 1.3: Scale of *Papilio palinurus* butterfly: TEM micrograph of a cross-section and top-view SEM micrograph (inset) [5].

All the measurements were performed with dry scales in air, or scales immersed in IPA. The authors also measured the index of refraction of chitin, the material of which the cuticle is made, and reported an average value of $N = 1.56 + i0.06$ over the visible spectrum, in agreement for the real part with Land [8]. As previously mentioned, it is believed that the presence of melanin in the scale structure is limited to the inner parts [19] or the innermost layers of multilayers [20]. Hence the imaginary part of the index of refraction, which describes the absorption of light by the material *i.e.* its melanin component, has to be regarded as an average over the whole scale volume. In another publication, Vukusic *et al.* [16] also reported on the reflectivity of the wings of two class II butterflies for normally incident ultraviolet and visible light. Mann *et al.* [18] performed high-resolution and large-aperture measurements on the wing of a specimen of *Morpho menelaus* (class I). They observed that the peak intensity of the reflected light and its spectral content varied substantially depending on the imaging location of their microscope setup.

Other mentioned publications present mainly structural and theoretical studies. Advances in electron microscopy have permitted us to render with increasing accuracy the minute features on the scales of butterflies, and have therefore fuelled a large number of structural studies. This improvement of our knowledge of the internal structure of the scales has been essential for the development of models to explain the qualitative and quantitative properties of the interaction between light and these structures. A review of models which have been proposed to explain the observed behaviour is presented in the following section.

Amongst butterflies of the first class, the species *Morpho rhetenor* shows the most dramatic effects and has the most intricate structure. For these reasons it has been the subject of several theoretical investigations and models have been drawn from the structural studies. The taxonomical designation of this species is reported in table 1.2. Specimens have been encountered in Peru, Surinam and Guyana.

Table 1.2: Taxonomical designation of *Morpho rhetenor* butterflies [23].

Order	*Lepidoptera*
Suborder	*Papilionoidea*
Family	*Nymphalidae*
Subfamily	*Morphinae*
Genus	*Morpho*
Species	*Morpho rhetenor*

The wings of *M. rhetenor* [17] are tiled with a single layer of blue scales. These scales are typically $75\mu m$ by $200\mu m$ in size. On the upper surface they have a longitudinal ridging with an in-plane periodicity of $(675\pm75)nm$. The ridges have a pine-tree cross-sectional shape as shown in figure 1.2, with ten branches attached on both sides to a central stem, horizontal and regularly ordered, with a vertical thickness of about $90nm$. The thickness of the air interstices is also about $90nm$, which results in an average periodicity of $180nm$. The trees are wide with respect to the in-plane periodicity and the cuticle material (chitin) fills approximately 30% of the volume occupied by the structure. The lamellae forming the branches of the tree structure are slanted along the direction of the ridges, with the angle of slant with respect to the plane of the wing at about 20° [19]. The lower side of the scale is featureless and plain.

Figures 1.4 to 1.7 show a *M. rhetenor* butterfly and views of its scales at different magnifications.

Figure 1.4: *Morpho rhetenor* butterfly (photo by Luca Plattner).

1.3 Models for the wing of butterflies

1.3.1 One-dimensional models

Modelling of the wing microstructure of butterflies as a one-dimensional system of alternating layers of cuticle and air has been used for almost a century. Land [8] in 1972 reports on studies from 1927 onwards and complies with the early observations and one-dimensional models.

Huxley [21] studied the reflectance of two class II butterflies and proposed a multilayer model with an angle-dependent index of refraction of air to account for the observed shift in wavelength of the reflectance maximum with varying angle of incidence. The author justified this model as a correction of initial approximations: that the presence of cuticle spacers in the air layers be ignored. Tada *et al.* [20] introduced the concept of *nonplanar specular reflection* while studying a class II butterfly, modelling the structure as a corrugated multilayer, thus accounting for the reflectance of their sample in certain parts of the investigated spectrum. Vukusic *et al.* [16] presented the issue of colour mixing by two *Urania*–type butterflies. Modelling the structure as areas of horizontal multilayer, which would appear yellow, and 45° tilted multilayer, which would appear blue, they quantitatively explained the green appearance of the wings at normal incidence.

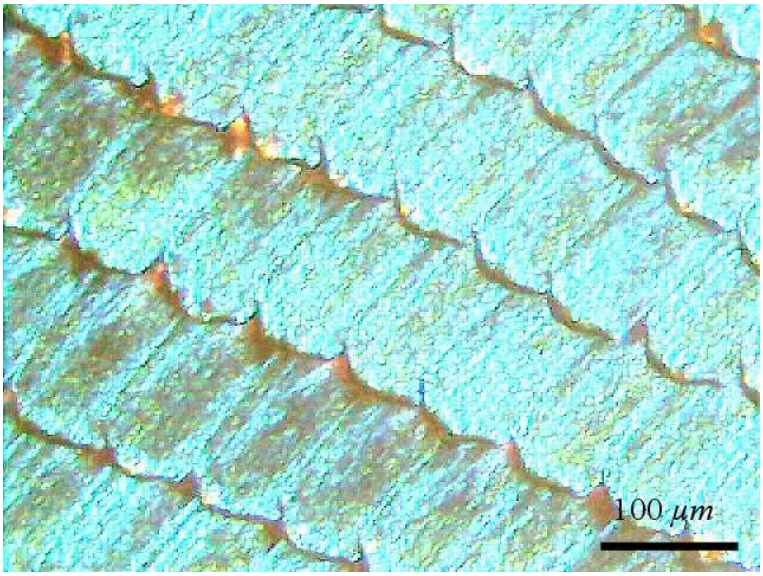

Figure 1.5: Wing of *Morpho rhetenor* butterfly: closeup of scales tiling (photo by Luca Plattner).

Ghirardella *et al.* [19], following in the footsteps of early researchers, discussed a simple thin-film model for the reflectivity of a butterfly in class I, *Eurema lisa*, which accounts for the shift in wavelength of the reflectance maximum with varying angle of incidence. Vukusic *et al.* [17] studied the optical properties of *M. rhetenor*, a butterfly in the first class. To explain the lobes found in the polar distribution of the backscattered light at $488nm$ and the reflectance across the visible spectrum for normal incidence they proposed a Gaussian distribution ($FWHM = 6°$) of multilayers around the $\pm 15°$ orientations from the wing normal. This model also agreed with Vukusic's measurement of the total reflection for normal incidence. Mann *et al.* [18] used a model with a multilayer of effective media to account for the varying width of the branches in the tree structure with depth and computed the reflectance of the structure. Their computations agreed with their measurements on the wing of a specimen of *Morpho menelaus* for wavelengths larger than $480nm$. All these models approximated the structure as a stack of thin-films, effectively a multilayer dielectric mirror.

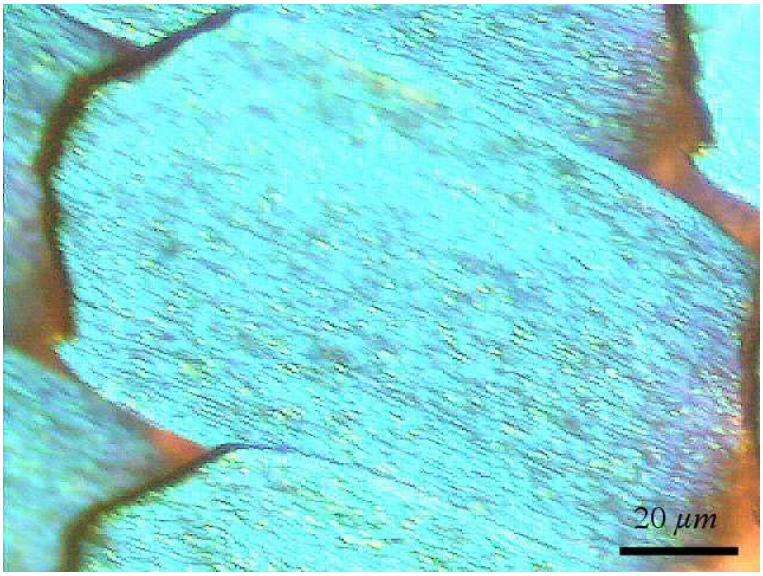

Figure 1.6: Scale of *Morpho rhetenor* butterfly (photo by Luca Plattner).

Although current models for the structures of both types might be improved, diffraction can, in general, be neglected for the structures of the second type due to the long periodicity of the ridged system. The reflection from this type of structures can be satisfactorily computed using the well-known methods of multilayer modelling. The optical properties of class I scales seem to be more difficult to explain, although several models have so far been proposed. These could only account for some of the optical effects and did not provide a complete explanation, as will be shown in later chapters.

1.3.2 Two-dimensional models

Modelling in two dimensions, a distribution of indexes of refraction in a plane is considered, with translational symmetry with respect to the normal to that plane. When considering the *Morpho* structure, this means that the *lateral* periodicity in the plane of the wing is accounted for in the model.

Cowan [24] showed that it is possible to obtain a blue reflection with a narrow bandwidth ($FWHM = 10\%$) from a coarse metallic multilevel grating.

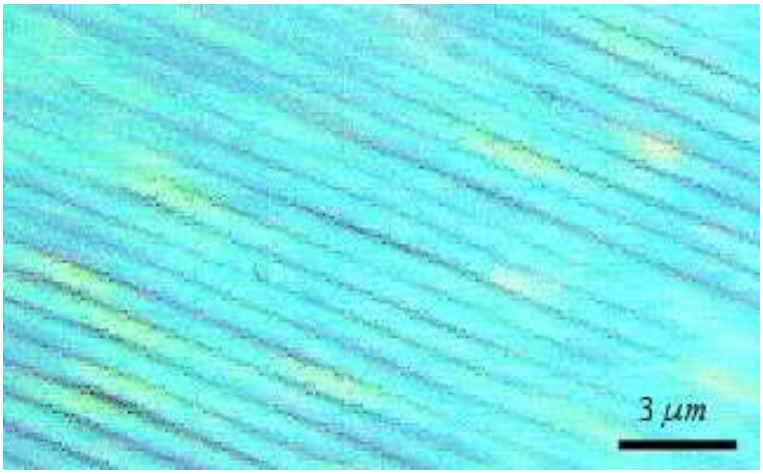

Figure 1.7: Scale of *Morpho rhetenor* butterfly: closeup of ridged structure (photo by Luca Plattner).

Using a scalar theory approach, the reflection of a periodic system of perfectly reflecting diffractive phase elements was studied, a structure inspired by the *Morpho* structure, which was called an *Aztec* grating. This is shown on the left hand side of figure 1.8 and consists of a symmetric multilevel binary grating (a pyramid of the Aztecs) with ten steps, the same number of branches on the ridges of the scales of *M. rhetenor*. Cowan's calculations did not depend on the lateral pitch of the grating and were valid only for wavelengths larger than several times the pitch. The peak wavelength of the reflected light at normal incidence was twice the height of the steps. The intensity of the diffracted orders was less than 30% that of the zero order with a direction of propagation dependent upon the chosen lateral pitch. It was demonstrated that a similar reflectance is obtained for asymmetric (blazed) diffraction elements (shown on the right hand side of figure 1.8), but the diffracted orders are much more intense.

Following recent advances in the modelling of gratings it has become clear that computation of the optical properties of surface-relief periodic structures, with pitches of the order of, or smaller than the wavelength of interest, cannot be accurately achieved other than by a rigorous solution of *Maxwell*'s equations. The structures on the scales of butterflies – particularly

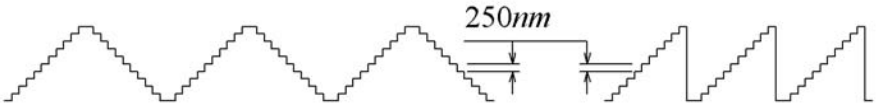

Figure 1.8: *Aztec* gratings modelled by Cowan [24]. Symmetric structure on the left hand side, blazed structure on the right.

if they belong to the first class – are no exception to this rule [9, 10].

Gralak *et al.* [25] reported a two-dimensional study of the appearance of a structure mimicking that of class I butterflies. The structure was composed of a central vertical stalk with 16 branches alternating on each side, in the fashion of a pine tree, periodically repeated in the horizontal plane. The lateral period was $746nm$, the distance between two subsequent branches on the same side was $207nm$ and the thickness of the branch layers $62nm$. The flat bottom of the scale sac was also included and the dielectric had an index of refraction $N = 1.56 + i0.06$. Using a rigorous modal theory, they simulated the colour of such a structure when illuminated incoherently from all upper directions and viewed at angles between the normal and 80° away from the normal. This simulation was performed for a structure in air, and one immersed in IPA to parallel the experiment of Vukusic *et al.* [17]. They also showed the spectra calculated for light incident at an angle of 45° with respect to the normal and on both sides of it. Finally, they presented plots of the field distribution within the structure for normally incident light.

1.4 Modelling multilayers

A multilayer is a stack of homogeneous thin-films with different indices of refraction and is usually modelled assuming that the arrangement of dielectric materials be invariant with respect to continuous translation in two orthogonal directions and not in the third.

The optical theory of thin-films was first presented in 1949 by Schuster [26]. The following year, Abelès [27] extended it to multilayers and for-

malized the computing technique called the *transfer matrix method* (TMM). The basic formalism yields the amplitude of the electromagnetic field of monochromatic waves reflected by and transmitted through the mentioned structure. The solution is achieved through propagation of the fields in the homogeneous layers, and the continuity of the tangential components of the electric and magnetic fields at the interfaces. Although the structure is one-dimensional, propagation for non-normal incidence can be accounted for. The solutions for plane waves are in fact vectors of the three-dimensional *Euclidean* space propagating in a plane. With the exception of approximations in the chosen model, *i.e.* simplified dimensionality and initial conditions, or neglect of material parameters, this analytical method is exact.

The optical properties of stacks of thin layers proposed by Hooke and Newton [1, 2] were confirmed by the TMM calculations, showing that multilayers are characterised by high reflectivity and transmissivity over large portions of the spectrum. Interest in a wide variety of important applications of multilayers, including antireflective coatings (AR), high reflectivity dielectric mirrors and filters, has prompted scientists to use the TMM to compute new designs. It has been demonstrated how to extend the spectral region of high reflectance [28], or the range of angles at which the desired effect occurs [29], and recent studies have presented the extension of the TMM to stacks of anisotropic materials [30, 31], showing how to obtain an omnidirectional reflector with existing materials.

The simple form of the TMM equations applied to a periodically stratified medium [32] is convenient for systems with a large number of layers, but novel developments in the study of periodic structures have offered new approaches for the investigation of periodic multilayers. These techniques involve decomposition of the field into periodic modes [33], and assume infinitely extended modulations of the index. These techniques therefore cannot model effects related to the finiteness of a multilayer or the interaction of light at its boundary with the incident medium, but they have proven powerful tools to investigate an important property of dielectric stacks: the photonic bandgap [34].

1.5 Modelling volume diffractive structures

Gratings have been the object of intense study ever since 18^{th} century scientists comprehended their usefulness in optics. More recently, advances in microfabrication have brought gratings back amongst the subjects of cutting-edge research. Together with the definition of features with smaller lateral size, deeper etching processes on one hand and stacking of periodic layers, called *multilevel* gratings, on the other, have allowed production of very deep structures with narrow pitches. Progress in holography has also permitted gratings to be produced with a previously unattainable depth. These structures have been termed *volume diffractive structures* after the name of their production technique [24]. Throughout the rest of this thesis we shall refer to volume diffractive structures as materials that besides having a surface capable of diffracting incident radiation, exhibit a distribution of index of refraction perpendicularly to their surface, deep within the structure.

A grating is traditionally an evenly spaced array of straight grooves on a planar surface, and is modelled as a distribution of material (dielectric or not) periodic in one direction and invariant with respect to continuous translation in the other. However, surface distributions periodic in two directions, found in Nature and which have also been fabricated, are often equally referred to as gratings.

With gratings, the ratio between the wavelength of the interacting light and the size of their features is a crucial quantity when modelling them. Depending on the wavelength-to-pitch and wavelength-to-depth ratios of an array of diffractive elements, differing computing techniques must be adopted. Gratings with large pitches compared to the operating wavelength are called *coarse*, while those with a small depth-to-period ratio are termed *shallow*.

1.5.1 Scalar methods

The scalar theory (ST) for diffraction gratings developed by *Kirchhoff* in the 19^{th} century [32] has been a very successful one, but it is accurate only for coarse and shallow gratings. Pommet *et al.* [35] showed that the accuracy of ST degrades with decreasing index of refraction of the grating material, with increasing deviation from the median filling fraction of 50%, and with increasing angle of incidence. Pommet *et al.* discussed quantitative criteria for the validity of the results of the ST: for one multilevel grating the results can be within a 5% accuracy only for wavelengths larger than 20 times the grating pitch at normal incidence. The structures considered by the authors are similar to the *Aztec* ones studied by Cowan [24], but they are dielectric and not perfect reflectors as in the latter case. Summarizing the two investigations, the lower wavelength threshold for the validity of the ST for an *Aztec* model of the type I butterfly structure is set beyond the long-wavelength edge of the visible spectrum for normal incidence and moves further away for larger angles of incidence.

1.5.2 Rigorous methods

Zero-order diffraction gratings are characterised by periods smaller than the operating wavelength and do not allow reflection or transmission of any diffraction order other than the fundamental one. Modelling of gratings with large wavelength-to-pitch ratios requires a rigorous solution of *Maxwell*'s equations. Assuming discrete translational symmetry and therefore infinite extension of the modulation, the fields decompose into periodic modes. A solution is obtained by expansion in the zone of the periodic distribution of index of refraction with periodic functions, and by energy conservation at its boundaries. The major difficulty with this method is to find a solution formulation for the scattering problem of a single diffraction element, which is also laterally periodic.

A method to rigorously obtain the diffraction of plane gratings with rectangular diffraction elements (lamellar gratings), the *rigorous modal method* (RMM), was proposed by Knop [36] and then formalized by Botten *et al.* [37]. With the RMM, an incoming plane wave is projected onto the *Fourier* basis functions and substituted into the *Helmholtz* equation. The incident field is separated into its components parallel and perpendicular to the plane of incidence and the problems for transverse electric (TE) and transverse magnetic (TM) polarisations are solved separately. With the simultaneous *Fourier* expansion of the dielectric function in the periodic medium zone, this yields a standard eigenvalue problem. The direction of propagation of the modes is obtained from the solution of the eigenvalue problem, the size of which depends on the order of truncation in the expansions, and the modes are successively propagated in the periodic medium. The tangential components of the fields for all the expansion orders are then matched at the boundaries between media (usually the isotropic incidence and substrate media, and layers of periodic arrangement of dielectric) and finally the amplitudes and phases of the diffracted waves are extracted. Although this rigorous technique is in principle applicable to diffractive elements of arbitrary shape, in practice the eigenvalue problem can only be obtained for lamellar gratings because of the limitation in finding a suitable solution formulation.

Moharam and Gaylord [38] proposed a similar method to RMM, which is called the *rigorous coupled-wave technique* (RCWT). It involves the same process of expansion of the fields and matching at interfaces between media, but the fields in the periodic medium are explicitly expressed and dependent on the coordinate normal to the grating plane. Consequently, the scattering problem of the arbitrarily shaped diffraction element is implicitly solved by the RCWT. This results in a set of coupled differential equations. In this case a standard eigenvalue problem is always obtained and for the same order of truncation its coefficient matrix has four times the number of elements than an RMM one.

For both methods, numerical instabilities in the solution of the TM problem result in poor convergence and therefore poor accuracy. The instabilities are related to the *Fourier* expansion of the dielectric constant and are referred to as *Gibbs* phenomena. Morph [39] showed that by using *Legendre* or *Chebyshev* polynomials, exponential convergence with increasing number of terms can be achieved, while with *Fourier* expansion the convergence is only linear.

1.5.3 Multilevel structures

Multilevel diffractive structures are stacks of lamellar gratings, therefore their optical properties can be computed using one of the rigorous methods discussed in the previous section. Multilevel gratings may either have the same period throughout all the layers, or varying period. If all the layers have the same period, RCWT can be used across the whole structure. Otherwise each layer has to be solved individually and the overall response is obtained by matching the tangential fields between layers. Using RMM, the problem always needs solving layer by layer.

Matching of the fields at the interface between layers, including incident and substrate media, is achieved with a method similar to the one-dimensional TMM discussed in section 1.4. The propagation matrices have the same size as those of the eigenvalue problems within the periodic layers. However, propagation of the incident fields throughout the layers by a transfer matrix (*T-matrix*) approach proved inaccurate, even in cases where good overall convergence was reached. This was due to backscattering exponentials with large positive and negative exponents causing numerical overflow [40]. Methods have been devised to eliminate this effect, which relate the fields in the isotropic media to those in each layer [40] (*R-matrix*), solve the boundary conditions for all layers simultaneously [39], or propagate forward and backward travelling waves separately [41] (*S-matrix*).

Once accurate efficiencies have been obtained for systems with many layers, the RMM can also be used to solve gratings with an arbitrary shape

by approximating the diffraction element with a stack of thin slices, thus discretising its shape [40].

1.6 Photonic crystals

The exploitation of electronic crystals has been one of the most important revolutions in the history of engineering and has driven the development of modern physics as we know it. The quantum theories explaining the mechanics of electrons in different materials have been a source of inspiration for scientists investigating the interaction between photons and matter. Interest in controlling material radiation has resulted in the conception of a new class of materials capable of interacting with electromagnetic waves at a structural level: they are called *photonic crystals* or *photonic bandgap materials*.

Purcell [42] in 1946 indicated that spontaneous emission of radio waves from nuclear spin levels could be controlled by a dispersion of small metallic particles in a nuclear-magnetic material, which would create a resonant oscillator. In 1972 Bykov [43] considered that spontaneous emission of atoms at optical wavelengths could be reduced by placing them in a periodic lattice of dielectrics with pitches smaller than the radiation wavelength, thus avoiding decay of excited states through the presence of *opaque* bands for the transition radiation and consequent generation of a *dynamic state*. Despite the early studies, a widespread interest for these optical systems became established in the scientific community only after the independent publications of Yablonovitch [44] and John [45]. The former proposed an active layer embedded in a face-centered cubic crystal of periodic epitaxial layers iteratively grown and etched, while the latter discussed models for strong localization of photons in perturbed lattices of scatterers. Both these works addressed the engineering of a structured material exhibiting ranges of frequencies at which the propagation of electromagnetic waves is not allowed, so called *bandgaps*, and their employment in the emission control of optically active materials.

Since then, photonic crystals have become the object of intensive inves-

tigation by a vast community of scientists. In the past fifteen years the number of publications in this field has grown exponentially, leading to the publication of more than 2600 papers to date [46]. Consequently research has become diverse and very specialized, which makes the production of a generic overview of the published material perhaps a pointless exercise, and certainly a titanic one. The reader is referred to several journal special issues [47, 48, 49, 50, 51] and the PhD theses of Charlton [52] and Zoorob [53] for reviews of these ongoing developments. Moreover, a comprehensive and continually updated list of all published material is available in reference [46].

In the following sections a choice of subjects has been made. A discussion of the most important techniques used to model photonic crystals will be treated, and a review of two-dimensional photonic crystals fabricated by stacking of thin-films, and of three-dimensional ones designed to operate at optical wavelengths, will be presented.

1.6.1 Modelling photonic crystals

Photonic crystals are essentially bulk materials, because the occurrence of the bandgap depends, amongst other things, on the modulation of the index of refraction over a large number of periods. The search for efficient bandgap materials has prompted scientists to solve *Maxwell*'s equations within the periodic arrangement. Ho *et al.* [54] were the first to correctly predict the existence of a *complete bandgap* in a specific photonic crystal structure, *i.e.* a range of frequencies at which no propagation of waves is possible in any direction in the crystal. By means of a *plane wave expansion method* (PWM) they calculated the size of the bandgap for a diamond lattice of spheres, and established its dependence upon the dielectric contrast and filling fraction parameters. Ho *et al.* showed that a face-centered cubic lattice of spheres cannot have a complete bandgap. The PWM is a three-dimensional version of the *Fourier* expansion technique mentioned in section 1.5.2 when discussing the rigorous modal method. The same difficulties have to be addressed here as in the one-dimensional case of lamellar gratings, namely a solution for the

single scatterer must be found which is periodic along the crystal axes, and numerical instabilities are encountered due to *Gibb*'s phenomena. Analytical solutions are therefore only found for systems composed of spheres in space, and cylindrical or rectangular rods in a plane of the crystal. Convergence issues related to *Gibb*'s phenomena are addressed using different expansion bases, for example *supergaussian* functions [55]. Whichever the method of expansion used, the total number of terms is determined by the order of the truncation to the power of the number of dimensions in the problem. The requirements for computation in terms of storage memory and speed of processing grow exponentially with increasing dimensionality of the problem to solve. Arbitrarily shaped "atoms" require numerical integration over the unit cell of the crystal, which is again very demanding computationally and even places many low dimensional problems beyond reach. Nevertheless, advances in this field have produced numerical methods which reduce the computational obstacles. By means of iterative optimization of an approximative initial solution, through a parallel computing approach via block matrix diagonalisation, or implementing ingenuous numerical measures, such as smoothing the dielectric function [56], many previously unattainable numerical calculations have been successfully solved.

The PWM was adapted by Sakoda [57] to compute the diffraction of two-dimensional periodic bandgap materials with a finite thickness. Using a plane wave expansion in the direction of periodicity of the dielectric function and an arbitrary *Fourier* expansion normally to that same plane, diffracted fields were successively matched to the field expansions within the periodic medium. Predictions of the diffraction of triangular and square lattices of air rods in planar waveguides were obtained in this way with good accuracy [58, 59].

The vectorial *multiple-scattering theory* (MST) of electromagnetic waves is an adaptation of the scalar one for electrons and uses the *Korringa-Kohn-Rostocker* (KKR) method to calculate the band diagram of finite arrangements of spherical scatterers [60]. The dielectric is represented as a super-

position of the *Green*'s functions of the single scatterers, each expanded in terms of vector solid spherical harmonics (*Neumann* functions). This technique, when used on regular structures, is equivalent to the PWM except for the choice of the expansion basis, but offers the possibility to directly implement finite arrangements, disordered systems and defects. The use of *Neumann* functions results in faster convergence than the PWM as shown by Leung and Qiu [61] in a comparative study of two-dimensional photonic crystals.

Pendry *et al.* [62] suggested an approximative finite-element method (FEM) to solve *Maxwell*'s equations over a discrete mesh of points in a simple cubic lattice. For a fixed frequency Pendry *et al.* propagated fields in one of the orthogonal directions of the lattice by means of an approximate wave vector and, assuming a periodic distribution, Pendry *et al.* applied periodic boundary conditions in the planes normal to the propagation direction. This resulted in a two-dimensional transfer matrix method (TMM) for the real-space fields, which was successively upgraded to its *Fourier*-space form, to work in the resonance domain of frequencies, and was capable of fast and accurate calculation of the response of complex periodic structures [63, 64].

Another method to solve *Maxwell*'s equations on a discrete lattice of points in space is the finite-difference time-domain (FDTD) method. This method has a long history and has been used in a variety of applications which are reviewed in the book edited by Taflove [65]. In 1995 Chan *et al.* [66] were the first to apply this method to compute the band structure of photonic crystals and to prove its reliability in treating periodic structures of high complexity. The FDTD calculations are particularly useful for complicated structures because the memory and processing time requirements scale linearly with the number of grid-points included in the computation, allowing resolution of minute and intricate structures. With the FDTD method an initial field is propagated applying the governing equations in a first-order differential form, both in space and time, at all points in the grid in a succession of time steps. Different types of boundary conditions can be applied

including periodic ones, particularly useful for this type of system. The fields at selected points on the grid are finally *Fourier*-transformed from the time to the frequency domain such that observations on spectral content can be made. Ward and Pendry [67] extended the FDTD method to nonorthogonal meshes, proved that the approximation of the equations conserves energy just as the original ones, and showed how to obtain the *Green*'s function of a system. The FDTD method allows solution of the governing equations inside a periodic structure, but also outside at the same time, offering a tool to study the coupling of waves between different media or devices, and the diffraction or scattering of light.

1.6.2 Layered two-dimensional photonic crystals

Metallo-dielectric multilayer gratings have become important in soft x-ray optics over the past decade, to obtain enhanced diffraction efficiencies for a variety of applications. Dielectric lamellar gratings coated with multilayers, or in some cases lamellar gratings etched in multilayers, were designed to work in the plasmonic range of frequencies, where electromagnetic radiation is not absorbed by the metal. The layering functioned as a quarter-wave stack and the lateral distributions as diffraction gratings far from their resonance domains, since the grating pitches were at least two orders of magnitude larger than the stack period.

The use of form-birefringence for optical polarisers has also attracted much interest in recent years and zero-order multilayer gratings have been fabricated with this goal.

Reflective polarisers for operation in the visible were demonstrated by Yu [68], using a metallo-dielectric lamellar grating defined by nanoimprint lithography. A mold was produced in silicon by interference lithography, metal lift-off and CHF_3 reactive ion etching (RIE). At a temperature of $175°C$, the mold was pressed into a PMMA film deposited on a silica substrate and then separated after cooling, forming a lamellar grating of PMMA with a pitch of $190nm$ and ridges $70nm$ wide. A $70nm$-thick layer of metal

was e-beam evaporated to coat the troughs and crests of the dielectric grating. The device was characterised for reflection at normal incidence and showed large extinction ratios over a wide range of frequencies with a maximum exceeding 250 for the design wavelength of $633nm$.

Deguzman and Nordin [69] stacked two gratings with different pitches and ridges orientations: a wire grid polariser and a dielectric form-birefringent quarter-wave plate. They obtained by this technique circular polarisation filters designed to work in the middle infrared spectrum of frequencies. The lamellar grating (pitch $1\mu m$, filling fraction 0.64) is obtained in a silicon substrate by contact photolithography using an absorptive anti-reflection coating (ARC) and successive RIE of the resist in a helium and oxygen environment, evaporation and lift-off of a chrome masking layer. Finally, the metallic pattern is transferred into the silicon by a two-step RIE (CHF_3 and SF_6 first and CF_4 later) obtaining grooves $2\mu m$ deep. The dielectric grating was then filled and planarised with resist. A $160nm$-thick layer of molybdenum was deposited on the planarised dielectric grating sandwiched between a $100nm$-thick silicon dioxide layer to act as an etch-stop and an ARC. Standard interference lithography, metal mask lift-off and RIE processes followed to produce wire grid polarisers of different pitches and thicknesses.

Tyan *et al.* [70] fabricated and optically characterised all-dielectric, multilayer binary gratings designed as polarising beam-splitters at telecommunication infrared frequencies. The structures were fabricated by sputtering five alternated layers of silicon (thickness $0.13\mu m$) and silicon dioxide (thickness $0.26\mu m$) on a silicon dioxide substrate, definition of a grating (pitch $0.6\mu m$, filling fraction 0.5) in PMMA resist via e-beam lithography, deposition and lift-off of a chrome masking layer, reactive ion etching in a C_2F_6 and NF_3/CCl_2F_2 environment, and finally removal of the chrome mask by wet etch. The structure was slightly underetched with a total depth of the etch of about $1.16\mu m$ and the lamellae showed a certain degree of tapering. These deviations from the designed device were investigated theoretically and it was shown that the deviations can have dramatic effects on the polarisation

extinction ratio of the structure. The angular response of the structure in transmission and reflection for monochromatic incident light at $1.523\mu m$ was characterised and agreed with RCWT modelling results over a certain range of angles of incidence.

Lopez and Craighead [71] fabricated a structure similar to that by Tyan *et al.* Their device was designed to act as a quarter-wave plate at normal incidence and as an off-axis polarising beam splitter at a wavelength of $632.8nm$. A lamellar grating was etched through a $0.5\mu m$-thick stack of three layers (silicon nitride, dioxide, nitride) deposited on a silica substrate. Definition of the grating (pitch $0.6\mu m$, filling fraction 0.5) was achieved by means of electron-beam direct lithography, lift-off of an aluminium masking layer and reactive ion-etching in a CHF_3 environment. The principle of the device was proved experimentally and extinction ratios of greater than 20 and 10 were measured in transmission and reflection, respectively.

A new technique for the fabrication of distributed, layered dielectric materials for the visible range of frequencies was recently demonstrated by Sato *et al.* [72]. With this method, called *autocloning*, a lamellar grating is defined in a substrate using e-beam lithography and RIE, and then used as morphological seed for layers of titanium oxide (TiO_2) or tantalum pentaoxide (Ta_2O_5) and silicon dioxide sputtered in an alternating sequence on the substrate. A careful balance of sputter deposition and sputter etching allowed them to grow replicated layers with a sawtooth cross-section. Structures with a pitch of $0.18\mu m$ and a lamination period of $0.16\mu m$ were produced, which were composed of 17 layers and exhibited a sawtooth slope of more than $40°$. Figure 1.9 shows an SEM cross-section of one fabricated device.

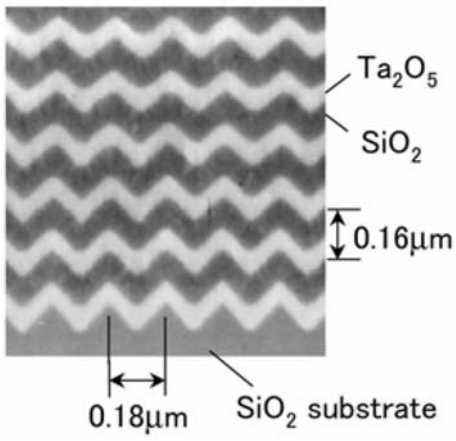

Figure 1.9: SEM cross-section of two-dimensional PC fabricated by Sato *et. al.* [72].

1.6.3 Three-dimensional photonic crystals for visible and near infrared regimes

In this section, a review of the published work regarding three-dimensional photonic crystals designed to operate at optical wavelengths in the visible and near infrared regimes of the spectrum is presented. Although numerous other contributions have been presented for larger scale structures, either as feasible demonstrators or as devices designed to operate in different regimes (microwaves or radio), research for optical devices in the visible and near infrared spectrum is particularly interesting on account of possible applications in the telecommunication technologies and for the manipulation of light. Moreover, producing such minute devices has proved extremely challenging with the available fabrication techniques, and research in this field is at the forefront of scientific engineering. Publications can be technologically categorized into three main areas: microelectronics and optoelectronics fabrication methods, holographic lithography and self-assembly processes.

Using the autocloning method [73] described in section 1.6.2 and employed by Sato *et al.* [72] to fabricate two-dimensional photonic crystals operating at visible wavelengths (see figure 1.9), Kuramochi *et al.* [74] produced a three-dimensional PC. It was produced using the same processes employed

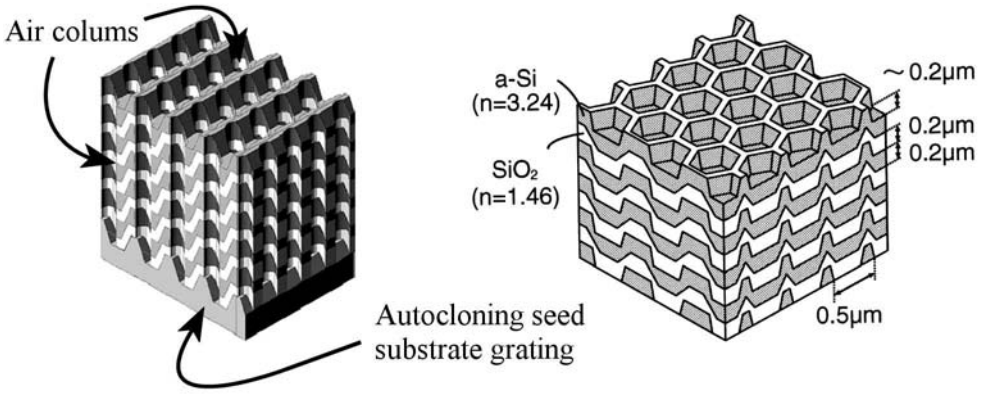

Figure 1.10: Schematic views of three-dimensional PCs fabricated by Kuramochi *et. al.* [74] (left-hand side) and Kawakami *et. al.* [73] (right-hand side).

for the above mentioned two-dimensional device, but was obtained from a different choice of alternating materials (amorphous silicon and silicon dioxide), and the implementation of different dimensions (lateral pitch $700nm$ and lamination period $320nm$) and total number of layers (12). In this two-dimensional layered grating, cylindrical air columns $300nm$ in diameter and $1\mu m$ in depth were etched by means of electron cyclotron resonance (ECR) etching, after e-beam lithography and metal mask liftoff. The columns were placed in a triangular lattice with a lattice constant of $404nm$ aligned to the ridges of the two-dimensional structure and centered in the middle of the sloping sides. A schematic view of the structure is shown on the left-hand side of figure 1.10. Kawakami *et al.* [73] fabricated another three-dimensional PC by applying the autocloning process with a seed defined on a triangular lattice with lattice constant $500nm$. Up to 20 pairs of amorphous silicon and silicon dioxide layers (thicknesses 200 and $120nm$ respectively) were stacked using this very stable process, resulting in the structure schematically shown on the right-hand side of figure 1.10.

Noda *et al.* [75] fabricated a three-dimensional PC with an asymmetric face-centered cubic crystal lattice (a *woodpile* structure) by defining lamellar

gratings of gallium arsenide or indium phosphide with a pitch of $675nm$ on two III-V semiconductor substrates. The grating lamellae were fabricated by electron beam lithography and dry-etching with an etch stop. The two substrates were then fused together in a hydrogen atmosphere with the two gratings stacked on each other with orthogonal orientations of the lamellae. One of the substrates and the relative etch-stop layer were eliminated by wet chemical etch to complete the process. This process can in principle be repeated several times, increasing the number of layers. A device was produced with four layers. Characterisation showed that the transmitted radiation was attenuated by up to $18dB$ at a wavelength of $1.1\mu m$ when compared with longer wavelengths.

Regarding holographic processes, a structure designed to operate at visible wavelengths was reported by Campbell *et al.* [76]. A $30\mu m$-thick resist layer deposited on a fused silica substrate was holographically structured using four non-planar laser beams. The source was an injection-seeded, frequency-tripled, Q-switched Nd:YAG laser producing $6ns$-wide pulses centered at $355nm$. After exposure, dissolution of weakly exposed resist resulted in high quality, single crystals of cross-linked polymer with face-centered or body-centered cubic structures and lattice constants ranging from 357 to $922nm$. The index of refraction of the polymer is approximately 1.6. An SEM view and a reconstruction of one fabricated device are shown in figure 1.11.

Multiple-component block copolymers undergo phase transitions between different self-assembled, periodic structures with lattice constants a few tens of nanometers in size depending on the volume fractions of the individual components. After annealing for prolonged periods of time, the structure exhibits the necessary morphological and mechanical stability. Fink *et al.* [77] used diblock copolymers like polystyrene/polyisoprene systems to produce self-assembled structures periodic in one, two and three dimensions with lattice constants of the order of $10 - 100nm$. Fink *et al.* demonstrated that, by applying external biasing forces during the phase transition, high

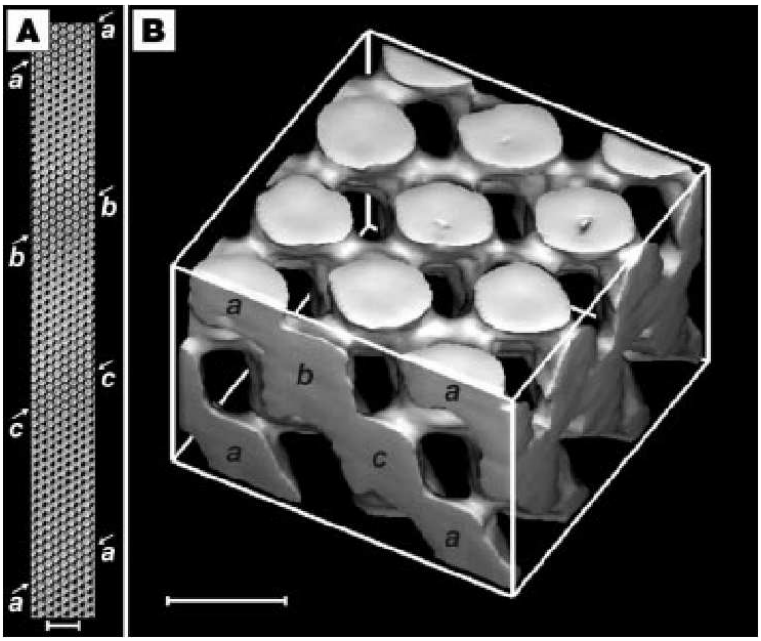

Figure 1.11: SEM view (left-hand side, A) and reconstruction (right-hand side, B) of a tree-dimensional PC fabricated by Campbell *et al.* [76]. Scale bars, $2\mu m$ (A) and $500nm$ (B).

quality structures could be obtained with large single-crystal domains. The major drawback when trying to generate PCs with this technique is that the contrast in refractive index, necessary to form bandgaps, is very low (the indexes of refraction of polystyrene and polyisoprene are 1.59 and 1.51, respectively). Optical characterization showed that effects related to the material band structure are noticeable and, even if limited, can be used under the right conditions to achieve interesting optical devices (*e.g.* the omnidirectional reflector discussed in section 1.4 [34]). A way to improve their optical properties is to selectively etch one of the components, thus leaving an interconnected PC of the other component in air, a process which has been demonstrated by the authors. Additionally, the resulting PC can be used as a template and filled with high index materials.

Amongst the self-assembly technologies for fabrication of three-dimensional PCs, the production of synthetic opals has been the most popular of approaches. By temperature-controlled settling of a colloidal suspension

containing monodisperse silica spheres with diameters chosen in the $200 - 1000nm$ range and synthesized using a sol-gel process, Míguez *et al.* [78] fabricated face-centered cubic lattices of close packed colloids. Mechanical stability and filling-fraction control (with filling fractions varying between 74 and 100%) was achieved by sintering (annealing) the sedimented solution. Due to the low index of refraction of the materials used and the high filling factors, only incomplete bandgaps (*pseudogaps*) can be obtained at this stage. By infilling the colloidal structure with indium phosphide, wide complete bandgaps were demonstrated.

Using a different method to order polystyrene colloidal particles $12\mu m$-thick, almost single-crystal structures in a hexagonal, close packed arrangement were achieved by Xia *et al.* [79]. An aqueous dispersion of the colloids was forced to flow through a flat cell which retained the self-arranging particles. That only pseudogaps can be achieved in this way is a theoretical fact. The authors however demonstrated that by using the colloidal structure as a template, filling its air gaps with a liquid precursor via capillary action, then curing the system with ultraviolet radiation or heat and finally etching away the template, a structure more likely to support large bandgaps can be fabricated.

1.7 Optical spectroscopy

New spectroscopic methods are being constantly developed in experimental optics as a fundamental part of the fast scientific evolution we have witnessed in the field of quantum optics. Detailed characterisation of the transmission and reflection properties of bulk and planar photonic crystal devices has been instrumental for the rapid advances achieved in this field. The importance of optical spectroscopy with out-of-plane sampling and collection of the diffracted radiation in the experimental study and the characterisation of the surface of periodic photonic structures has emerged in recent years. Investigations of the dispersion of photonic crystal waveguides have been re-

ported by Astratov *et. al.* [80] and Netti *et. al.* [81]. Advances in ultrafast laser physics and nonlinear optics have added to this experimental method a wealth of new opportunities. In fact, the availability of high-intensity femtosecond pulses, both very short in time and very wide in spectral bandwidth, provides the means to perform high resolution, time-resolved experimentation and to use coherent light containing a broad continuum of optical frequencies for spectroscopical analysis. This has also brought strategic advantages to steady-state experiments. Whereas before spectroscopy was limited by the availability of only discrete laser sources, requiring realignment when scanning a spectrum of frequencies, or low-power continuously tunable ones, unable to provide the light intensity necessary to quantify accurately the diffraction of highly dispersive materials, now it has become possible to take high-resolution snapshots of the light diffracted by the samples under investigation. This allows us to rigorously assess dispersive behaviour of sample areas just a few hundreds of nanometers in size, a quality instrumental to the experimental work carried out in the present study.

1.7.1 Supercontinuum generation

Supercontinuum (SC) generation is a nonlinear phenomenon characterised by dramatic spectral broadening of intense light pulses passing through a nonlinear material.

The development of lasers in the 1960s has provided sources capable of generating light intensities previously unknown to scientists. Through lasers with pulsed output it has become possible to measure and study nonlinear phenomena in the interaction between light and matter, which go undetected in the regimes achieved with incoherent light and continuously operated lasers. It is only when the field intensity is no longer negligible compared to the internal atomic fields (*i.e.* it is of the order of $10^6 Vm^{-1}$ or above) that, in general, the nonlinear terms of the polarisation field become experimentally appreciable. In nonlinear optics, a number of multiple wave interactions are used to describe the behaviour of the fields, which result in a

range of frequency generation and mixing processes. Consequently, phenomena like harmonic generation, parametric conversion or self-phase modulation are accounted for theoretically. Photons equally interact with material excitational waves, such as molecular vibration states and phonons, giving rise to additional frequency conversion processes. *Raman* scattering, *Brillouin* scattering and *Rayleigh* scattering are attributed to these interactions. The reader is referred to the classic book by Shen [82] for an extensive discussion of nonlinear processes and all the topics discussed in this section.

All these phenomena can contribute to the generation of an SC, but it is only achieved if the dispersion properties of the nonlinear material supports coherent processes along the optical path of the pulse. Until recently, the most effective media used for SC generation were nonlinear crystals, such as beta barium borate (BBO) or potassium titanil phosphate (KTP). The anisotropy of crystals provides the necessary geometrical asymmetry to exploit the second harmonic generation and their birefringence offers phase-matching conditions for coherent wave generation.

1.7.2 Supercontinuum generation in photonic crystal fibres

Recently, the use of photonic crystal fibres (PCFs) for SC generation has emerged as both very efficient and promising. Although fused silica, the building material of optical fibres, possesses a relatively low nonlinear susceptibility, PCFs are excellent nonlinear media because of their low loss and small effective area. A pulse of light can travel inside PCFs over long distances and the nonlinear effects arising from the highly confined field add up considerably.

SC generation in the visible regions using PCFs was first reported by Ranka *et al.* [83]. The authors studied the evolution of the SC generation with the increase of peak power, by coupling $100fs$ pulses with a center wavelength of $770nm$ and peak powers of $20W$, $220W$ and $1.6kW$ into a $10cm$-long PCF. The microstructured fibre consisted of a slightly elliptical

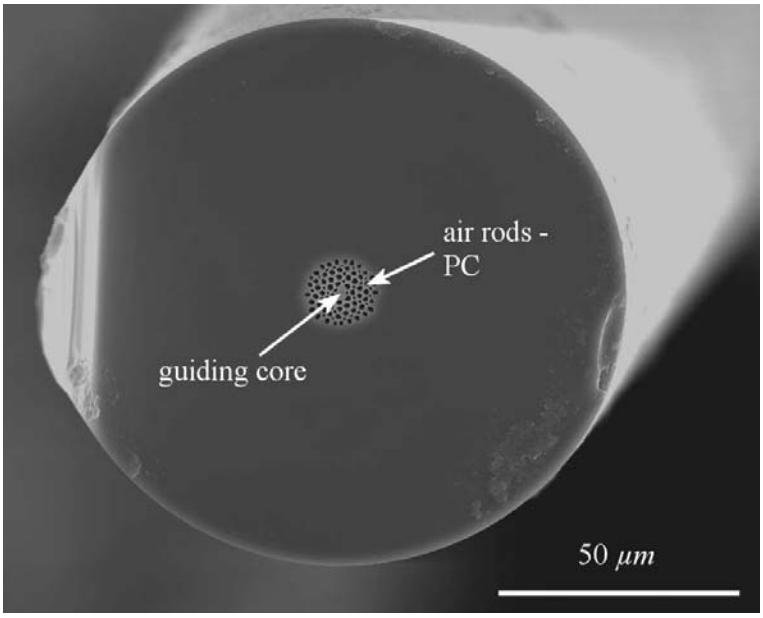

Figure 1.12: SEM cross-sectional view of silica photonic crystal fibre without external cladding (courtesy of W. Belardi, ORC, University of Southampton [87]).

$1.7\mu m$-diameter silica core surrounded by an array of $1.3\mu m$-diameter air holes in an hexagonal close packed arrangement, not qualitatively dissimilar from the fibre shown in figure 1.12. The background loss of the fibre was measured to be $50dB/km$ at $1\mu m$ wavelengths. The bandwidth of the output grew with increasing power to reach more than $500nm$. When injecting into $75cm$ of the same fibre a $100fs$ pulse centered around $790nm$ with a peak power of $8kW$, they obtained an SC varying by less than two orders of magnitude over the 430 to $1500nm$ range of wavelengths.

The fundamental property exhibited by PCFs which enables them to support SC generation is their characteristic anomalous dispersion in the visible range [84]. In bulk silica, the zero group-velocity dispersion wavelength occurs at around $1.3\mu m$, but the dispersion properties of the fibre due to the PC microstructure cause this parameter to shift to shorter wavelengths and eventually to the visible for small enough core diameters.

Coen *et. al.* [85] showed that an SC could also be obtained pumping a

PCF ($10m$-long with a $1.6\mu m$-diameter core) with a relatively long pulse of $60ps$ and $1.5kW$ peak power, centered at $647nm$.

The physical phenomena involved in the generation of SC in PCFs are still much the subject of debate within the scientific community, but an experimental and numerical study by Genty *et. al.* [86] showed that the relevance of various mechanisms in the formation of a continuum critically depends on the pump wavelength. In their extensive theoretical analysis they showed that, when pumping in the anomalous dispersion regime, high order soliton splitting due to *Raman* scattering and higher-order nonlinearities initiate SC generation by forming red-shifted solitons. These then radiate phase-matched, blue-shifted light in the normal dispersion regime. Due to the fibre dispersion, the center frequencies of the solitons undergo a gradual red-shift while travelling and also a self-phase modulation, both of which are transferred to their radiated components. Finally, four-wave mixing of the soliton frequencies also plays a role and assists in closing the gaps in the spectrum. Until the pump energy has been depleted by nonlinear conversions along its propagation path, it is the addition of all these continuously produced components that results in an output with a very wide spectrum. Pump wavelength, pump power and fibre length all affect the SC spectral content.

Price *et. al.* [87] demonstrated ultra-broad SC generation from a PCF seeded with a diode-pumped, ytterbium-doped fibre laser, successively amplified with fibre amplifiers. The seed, a $350fs$-long pulse with a centre wavelength of about $1050nm$ and a peak power of $20kW$, was launched into $7m$ of their PCF (shown in figure 1.12 and possessing losses of approximatively $100dB/km$ at the seed centre wavelength). The output was an ultra-broad spectrum spanning from just above $400nm$ to $1750nm$, varying in intensity by less than two orders. The setup consisted of a highly efficient all-fibre white-light source, whereby the bulky systems traditionally used to generate femtosecond pulses for SC generation were avoided.

1.8 Conclusion

The subject of this study, its scientific interest and relevance to the fields of zoology and optical engineering were presented in this chapter.

From a survey of the published material, it emerged that a complete experimental investigation of the optical properties of the *Morpho* microstructure has not been reported yet. The measurement of the scattering properties of the microstructure has been a central factor to this study and will be reported in chapter 4. Photonic crystal fibers have been instrumental to obtain these experimental data owing to their capacity to generate coherent, white light for spectroscopy purposes. A review of the published material in this germinal field of optics has been presented here.

The morphology of the *Morpho* microstructure suggests that previous models of its interaction with light are too simplistic, despite agreeing with the experimental data so far collected. The results of our experimental work confirmed this view. The two-dimensional nature of the periodic arrangement requires a model including the modulation of index of refraction in two orthogonal directions, similar to those employed for the modelling of volume diffractive structures, such as multilevel gratings and photonic crystals.

For the theoretical investigation of the optical properties of volume diffractive structures, it is necessary to use a rigorous, full-vectorial theory. Several methods to compute the diffraction of such structures have been developed in the fields of diffractive optics and photonic crystals. The assumptions and limitations of these methods were discussed. The theoretical study of periodic structures drawn from the *Morpho* microstructure is presented later in this thesis. The use of the plane wave method to investigate the band structure of these arrangements is reported in chapter 2, while the finite-difference time-domain method was used to compute their diffraction as reported in chapter 5. The contribution of those structures for the mechanism of colour production on the wings of *Morpho rhetenor* is discussed in chapter 6.

Published material on the fabrication of layered two-dimensional photonic crystal structures and of three-dimensional photonic crystals operating at

visible and near-infrared wavelength, was also presented with the intention to provide an overview of the available technologies and material for comparison with the fabrication work presented in this thesis. All known reported devices in these categories and their fabrication have been discussed. The fabrication of volume diffractive structures inspired by the *Morpho* microstructure will be presented in chapter 3.